DSC Annealing Study of Microphase Separation and Multiple Endothermic Behavior in Polyether-Based Polyurethane Block Copolymers

Louis M. Leung† and Jeffrey T. Koberstein*

Polymer Materials Program, Department of Chemical Engineering, Princeton University, Princeton, New Jersey 08544. *Received March 22, 1985*

ABSTRACT: The effect of thermal annealing on multiple endothermic behavior and microphase separation in polyurethane elastomers has been studied by differential scanning calorimetry (DSC). Measurements of the soft-microphase glass-transition temperature (T_g) and change in heat capacity (ΔC_p) at T_g are reported for various thermal annealing treatments and are used to construct a composition–temperature diagram. The resultant diagram demonstrates that the materials undergo a microphase separation transition (MST) which involves the disruption of microdomain structure to form a homogeneous mixed phase. Melt quenching experiments confirm that the melt phase at 240 °C for these elastomers is homogeneous. Thermal annealing–quenching experiments are used to map out the peak temperatures of multiple endotherms as a function of annealing temperature and specimen composition. Three characteristic endotherms are observed in the DSC thermograms. A time-dependent low-temperature endotherm is found at temperatures 20–40 °C above the annealing temperature. An endotherm observed at intermediate temperatures (140–210 °C) is shown to be associated with the onset of the MST process. The apparent MST temperatures are found to increase with the hard-segment content. In crystallizable materials, a third high-temperature endotherm appears due to melting of microcrystalline hard segments. The peak temperatures of the three characteristic endotherms are sensitive to small changes in the annealing temperature and depend upon sample composition. The general peak endotherm temperature behavior is discussed in terms of differences in the average hard-segment sequence length and changes in the thermal and morphological environments for crystallization.

Introduction

The elastomeric properties of segmented polyurethane block copolymers result from the microphase separation that is manifest between "incompatible" rubbery soft-segment and glassy hard-segment sequences. The glassy hard microdomains act as thermally labile physical cross-link sites as well as fillers for the rubbery soft-segment matrix. A large number of previous investigations have reported on the characterization of this microdomain structure using a wide variety of experimental techniques.

The majority of previous work concentrated on the determination of the degree of microphase separation, either through the application of small-angle X-ray scattering analyses (SAXS)[1-9] or by analysis of the soft-microphase glass-transition temperature obtained from dynamic mechanical[10-18] and differential scanning calorimetry (DSC) measurements.[19-26] The general conclusion of these studies has been that microphase separation is not complete. In most cases, an elevation in the soft-microphase glass-transition temperature is observed as a result of the presence of "dissolved" hard segment. In addition, the dissolution of a hard-segment sequence lowers the effective filler content and leads to a loss of two physical cross-link sites for the soft segment at the microdomain interface. These effects consequently affect the modulus of the material. Although quantitative analysis of T_g behavior has appeared,[24,25] the complete description of microdomain mixing from DSC measurements has been hampered by the lack of data regarding T_g of the hard microdomain and the heat capacity change at T_g, ΔC_p.

Quantitative determination of microphase compositions by SAXS has been plagued by similar problems. SAXS invariant calculations show clearly that microphase separation is incomplete but cannot specify values for compositions of the individual domains, as was pointed out by Bonart et al.[1,2] We have shown recently that the results of soft-microphase T_g analysis coupled with SAXS measurements can be useful in this respect, demonstrating that both the hard and soft microphases are mixed.[6]

Another important aspect of the microphase behavior that remains unresolved is the morphological origin of apparent multiple melting endotherms observed in certain polyurethanes. Three endotherms are generally observed. A low-temperature endotherm observed 20–40 °C above the annealing temperature has been ascribed to short-range reorganization within the hard microdomains. Intermediate-temperature endotherms observed below 200 °C are generally attributed to the disruption of long-range order of an unspecified nature. Finally, an endotherm occurring above 200 °C is typically assigned to the melting of microcrystalline regions of hard microdomains, although well-defined crystalline wide-angle X-ray diffraction is usually absent. DSC studies have shown that the temperatures and enthalpies associated with these endotherms are sensitive to changes in the thermal history and annealing conditions.[20,22,26]

Recently, we described a SAXS investigation of the microdomain mixing and morphology of a series of polyether polyurethane block copolymers.[6] In this article, we present the results of detailed DSC studies of the thermal transition behavior of this same series of materials as a function of hard-segment content and annealing conditions. This information is used to probe the time- and temperature-induced changes in polyurethane microdomain composition and morphology.

Experimental Section

A series of segmented polyurethane block copolymers with varying hard-segment content are studied. The hard segments consist of 4,4′-methylenediphenyl diisocyanate (MDI) chain extended with butanediol (BD). The soft segment is poly(oxypropylene) end-capped with 30.4 wt % oxyethylene (M_n = 2000, functionality = 1.94). Schematic chemical representations for the hard- and soft-segment units are shown in Figure 1. The polymers are prepared by a one-step bulk polymerization process with 4% excess MDI to ensure complete reaction. Details of the polymeriztion procedures may be found elsewhere.[16] The notation used for this series of polymers is PU–XX, where XX represents the weight fraction of hard segment. The chemical compositions of the materials studied are presented in Table I along with some

* To whom correspondence should be addressed.
† Present address: Department of Polymer Science and Engineering, University of Massachusetts, Amherst, MA 01003.

0024-9297/86/2219-0706$01.50/0

Table I
Characteristics of Elastomers

materials	hard segment, wt % (MDI + BDO)	density, g/cc	av MW[a] of hard segment, g/mol of HS	no. MDI per hard segment[a]	hard segment theoretical volume fraction
PU-20	20	1.142	500	1.7	0.17
PU-30	30	1.165	900	2.8	0.26
PU-40	40	1.192	1400	4.2	0.35
PU-50	50	1.218	2000	6.2	0.45
PU-60	60	1.235	3100	9.2	0.55
PU-70	70	1.270	4800	14.1	0.66
PU-80	80	1.292	8100	24.0	0.77

[a] Calculated from the most probable distribution for a one-step polymerization.[46]

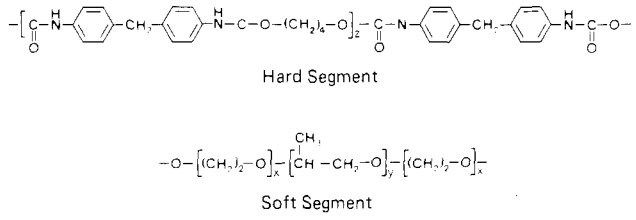

Figure 1. Structural schematics of hard- and soft-segment moieties.

associated physical characteristics. Specimens are reprecipitated from solutions of the "as-received" polymers,[6] dried, and then molded into 2-mm-thick, 1.5-in.-diameter disks at 180 °C and 3000 psi for 5 min under vacuum. The mass densities of the molded specimens are determined by the buoyancy method in heptane. The theoretical volume fraction of hard segment is then calculated from the chemical composition with the assumption of complete phase separation and volume additivity. The soft-segment prepolymer mass density employed in this calculation is measured pycnometrically.

DSC data are obtained with a Perkin-Elmer DSC-4 equipped with a data station. All thermograms are base-line corrected, normalized to sample weight, and calibrated by using indium and sapphire. Experimental specimens are cut from the molded disks and range in size from 10 to 15 mg. The scan rates employed are 20 and 40 °C/min. All measurements are carried out under a dried helium purge. Transition temperatures are corrected for the scan rate[27] and deviation from the indium calibration. Due to the presence of multiple endotherms, the reported apparent melting temperatures (T_m) are peak temperatures. Glass-transition temperatures are reported for both the onset and the midpoint of the glass-transition process. In quench-mixing studies, the copolymers are first heated to 240 °C (above the highest endothermic transition exhibited by the copolymers) and held at that temperature for 1 min. This is followed by quenching to −120 °C at the maximum DSC programming rate (320 °C/min). The quench-mixed samples prepared in this fashion are heated to 150 °C at 20 °C/min and then cooled to −120 °C at the same rate to complete the thermal cycle.

Specimens for annealing studies are held at 240 °C for 1 min and then cooled at 10 °C/min to the prescribed annealing temperature. The sample is annealed isothermally at this temperature for a fixed time period and then quenched at the maximum cooling rate. The sample is kept at the quench temperature (−45 °C with the intracooler and −120 °C with liquid nitrogen as coolant) for 5 min and subsequently heated to 240 °C at the selected heating rate. Degradation or changes in sample composition are monitored with a control sample. For most of the samples, more than 95% of the polymer can be recovered by reprecipitation from filtered dimethylformamide solution following annealing, indicating that significant cross-linking or allophanate formation does not occur.[6]

Results and Discussion

Quench Mixing. In order to study annealing-induced morphological changes, it is imperative to first establish a reference state or thermal pretreatment cycle wherein all memory of prior thermal history is erased. In the case of polyurethanes, such a pretreatment necessarily involves the complete disruption of all crystalline and/or micro-

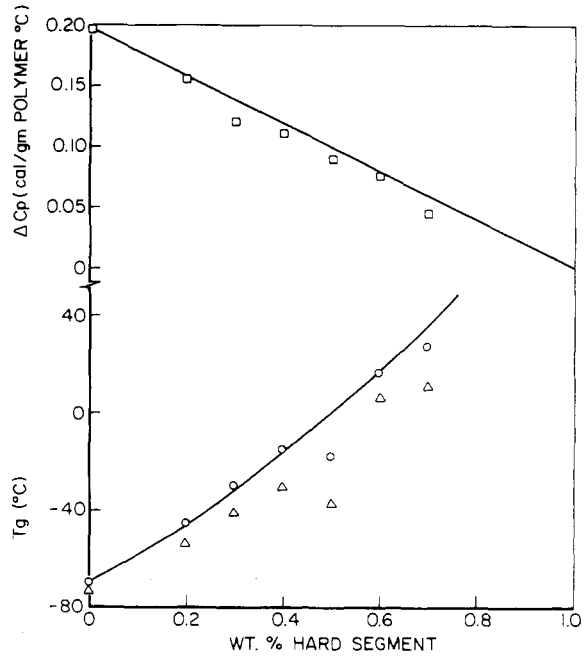

Figure 2. Soft-microphase glass-transition temperature and heat capacity change for polyol and melt-quenched elastomers: (△) T_g onset; (○) T_g midpoint; (□) ΔC_p. The solid line on the upper curve indicates ΔC_p values for ideal microphase separation of the soft segment. The solid line on the lower curve denotes the best fit of eq 1.

domain structure. The temperature of the preconditioning step must therefore exceed both the highest melting temperature and the temperature of the microphase separation transition (MST). The MST is the temperature at which microphase separation from the homogeneous phase occurs. The conditions necessary to attain a homogeneous melt state are identified by performing quench-mixing studies. The specimen is held at elevated temperatures for a set period of time and then rapidly quenched in order to "freeze in" the morphology present at that temperature. If a homogeneous melt is attained at that temperature and the quench is sufficiently rapid to avoid significant phase separation, the resultant frozen-in mixed phase exhibits a single glass transition. The associated temperature (T_g) and heat capacity change (ΔC_p) of this transition are then related only to the chemical composition of the sample and the pure component thermal properties. The results of quench-mixing experiments on samples conditioned at 240 °C for 1 min are summarized in Figure 2.

The solid line on the T_g curve corresponds to a best fit of a generalized Fox equation[28] assuming complete mixing of hard and soft segments

$$\frac{W_{SS} + kW_{HS}}{T_g} = \frac{W_{SS}}{T_g^0{}_{SS}} + k\frac{W_{HS}}{T_g^0{}_{HS}} \qquad (1)$$

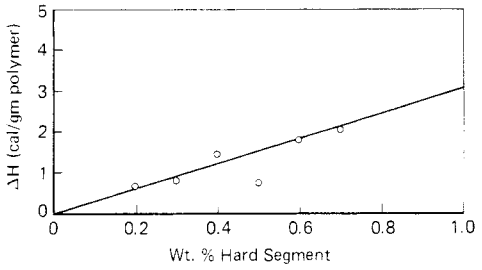

Figure 3. Experimental exotherm enthalpies observed upon reheating melt-quenched elastomers.

where the Wood constant k is unity in the original treatment.[29] The subscripts SS and HS refer to the soft segment and hard segment, respectively; W is a weight fraction; the superscript 0 denotes pure constituent values; and T_g is the experimental value. The two weight fractions required for fitting this relation are obtained from the known chemical compositions of the samples (Table I), and ${T_g}^0_{SS}$ is assumed to be equal to the measured glass-transition temperature of the soft-segment prepolymer (−69 °C). k and ${T_g}^0_{HS}$ are subsequently determined from the slope and intercept of the linear-least-squares fit to eq 1. The best fit gives $k \simeq 1.18$ (excluding the data for PU-50 and PU-70) and extrapolates to ${T_g}^0_{HS} = 109$ °C. This is in agreement with the reported value of 110 °C for MDI–BD,[30] supporting the supposition that the melts at 240 °C are homogeneous.

The ΔC_p behavior of the quenched-mixed specimens is also shown in Figure 2. If a single homogenous phase is present, the total ΔC_p is given by the linear weighted combination of the pure constituent values[31]

$$\Delta C_{p,mix} = W_{HS}\Delta {C_p}^0_{HS} + W_{SS}\Delta {C_p}^0_{SS} \qquad (2)$$

A fit of the ΔC_p data to this relation yields $\Delta {C_p}^0_{SS} = 0.194$ cal/g and $\Delta {C_p}^0_{HS} = -0.02$ cal/g. The soft-segment value agrees well with the measured value of the soft-segment polyol (0.195 cal/g). Within experimental error $\Delta {C_p}^0_{HS}$ is effectively 0 for MDI–BD, as has been suggested by Camberlin and Pascault.[24]

This result is in apparent conflict, however, with the T_g behavior that was well described by the modified Fox equation. Couchman[31] has discussed the derivation of (1) and shown that k is related to the ratio of ΔC_p values for the pure components (i.e., hard and soft segments). The fact that k is found to be of the order of unity suggests that $\Delta {C_p}^0_{HS}$ should be finite and roughly equivalent to $\Delta {C_p}^0_{SS}$. In additon, the observation that $\Delta {C_p}^0_{HS} \simeq 0$ is not consistent with the Simha–Boyer rule[32] which predicts that $\Delta {C_p}^0_{HS} \simeq 0.07$ cal/g.

One possible explanation for this discrepancy is the occurrence of a small amount of phase separation during quenching. This would have the effect of lowering the measured ΔC_p and would lead to an overestimate in k. This is currently being examined by small-angle X-ray scattering characterization of the quenched-mixed specimens. At present, however, the apparent conflict in ΔC_p data remains unresolved.

Upon heating above Tg, the quench-mixed samples spontaneously microphase separate, as indicated by an exothermic process in the DSC thermogram. The onset temperatures for these exotherms occur 40–80 °C above the homogeneous phase T_g (melt-quenched) and show no distinct trend with temperature. The microphase separation enthalpies are plotted in Figure 3. The extrapolated value for pure hard segment is ca. 3 cal/g (excluding PU-80, which may have crystallized), corresponding to an association enthalpy of approximately 0.5 kcal/mol of NH

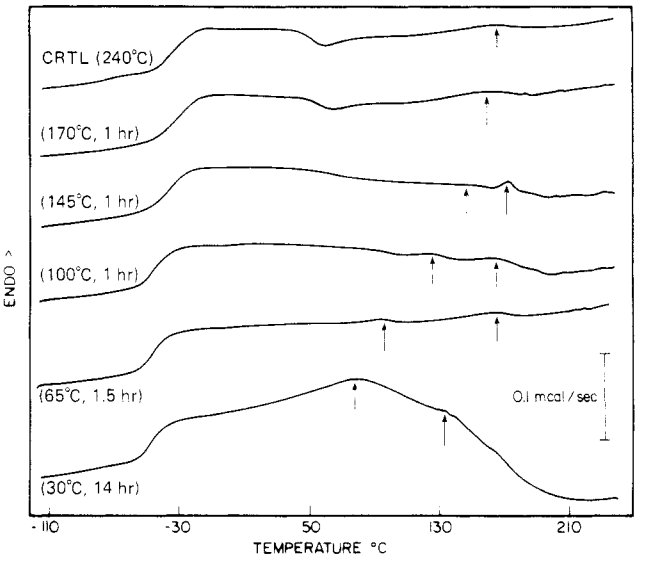

Figure 4. PU-30 thermograms as a function of annealing temperature.

units if complete hydrogen bonding is assumed (two hydrogen bonds per hard segment unit). This is considerably lower than values of 7.5 kcal/mol NH[33] and 6.6 kcal/mol NH (calculated from the data in ref 19) determined by infrared hydrogen bond dissociation measurements. A smaller experimental value is to be expected in our experiments wherein neither complete microphase separation of all of the hard segment units nor complete hydrogen bonding is attained. (A substantial fraction of the hard segment units resides either within the soft microphase or within the diffuse microphase boundary.[6]) In addition, a recent article has cast some doubt as to the validity of these hydrogen bond dissociation measurements.[34] The occurrence of some phase separation during quenching would also tend to decrease the observed demixing enthalpy.

The bulk of the experimental evidence therefore supports the conclusion that the copolymer melts (at 240 °C) exist in a homogeneous mixed phase, as has been found in other MDI–BD polyurethane systems by Wilkes et al.[35-38] A temperature cycle up to 240 °C is thus applied prior to all annealing treatments in order to eliminate the influence of prior thermal conditions. The specimens are held at this temperature for ca. 1 min.

The sample reheating is continued beyond the exotherm liberation up to a temperature of 150 °C, at which time the sample is cooled at 20 °C/min. The glass-transition temperatures measured during this cooling cycle (and upon a subsequent reheat) are all lower than those for the homogeneous melt-quenched samples, confirming that demixing occurs below 150 °C. The results clearly show that the materials are homogeneous at 240 °C but microphase separate below 150 °C. The following section presents a series of annealing studies aimed at further probing the details of the microphase separation and multiple endothermic behavior of these polyurethanes.

Annealing Behavior. Annealing studies are carried out for three selected samples, PU-30, PU-50, and PU-70. These samples vary in hard-segment content and therefore have different hard-segment sequence-length distributions. In addition, the hard-microdomain morphology is discrete for PU-30, but continuous for PU-50 and PU-70, as evidenced in previous SAXS studies.[6]

A. PU-30 Annealing Study. DSC thermograms (20 °C/min) for PU-30 are shown in Figure 4 for annealing temperatures (T_a) of 30, 65, 100, 145, and 170 °C. Only weak endotherms are observed under all annealing con-

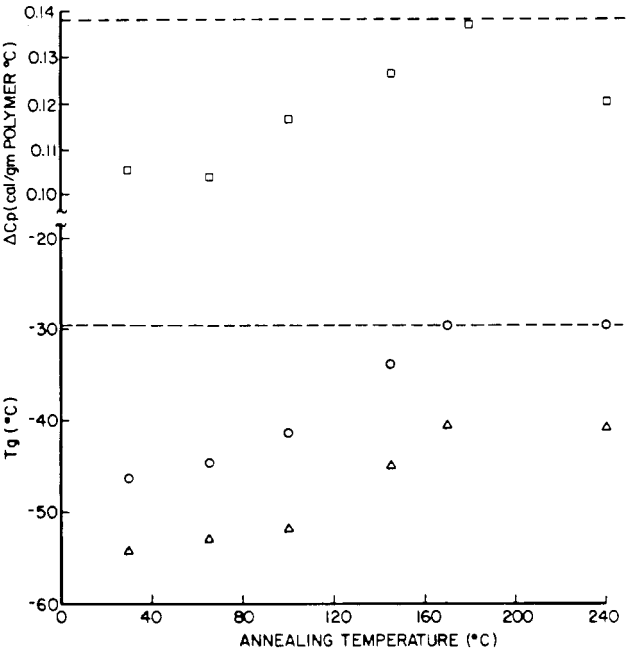

Figure 5. PU-30 soft-microphase glass-transition temperature and change in heat capacity as a function of annealing temperature: (□) ΔC_p; (△) T_g onset; (○) T_g midpoint. The dashed lines represent values for the completely disordered phase taken from Figure 2.

ditions for this material, consistent with the previous conclusion that the hard-microdomain structure is poorly developed.[6]

Measurements of the soft microphase ΔC_p and T_g are carried out for these annealing treatments and are reported in Figure 5. The T_g increases and broadens with increase in T_a, reaching a maximum for T_a = 170 °C. Annealing above 170 °C does not affect the transition temperature, demonstrating that the microdomain structure is completely disordered above this temperature. The ΔC_p value for the sample annealed at T_a = 170 °C supports this conclusion in that it is equivalent to the maximum value attainable when all the soft-segment material takes part in the transition process.

The measured ΔC_p increases for annealing temperatures below 170 °C, indicating that the overall fraction of soft-segment material residing in the soft microphase also increases. The low value of ΔC_p for $T_a \sim 80$ °C and below implies that a substantial fraction of the soft-segment units are mixed within the hard microdomain, perhaps trapped in at the hard microdomain T_g (expected at ~80 °C). Below T_a = 80 °C the ΔC_p is constant, yet T_g increases with increase in T_a. Previous investigators also observed this behavior.[38] They attributed the T_g elevation to contractile forces generated in the rubbery soft segments as the temperature is increased. These forces induce further mixing by pulling additional hard segments into the soft microphase. The ΔC_p, however, is relatively unaffected by this process since $\Delta C_p{}^0{}_{HS}$ is effectively 0.

An approximate microphase composition–temperature diagram may be constructed by further analysis of this data. The composition of the soft-segment-rich microphase ($W_{1,HS}$) is calculated by application of eq 1, using the parameters obtained from best fit in Figure 2 and the measured T_g of the soft micrphase. The hard-segment-rich microphase composition is then calculated by application of the lever rule leading to

$$W_{2,HS} = \frac{W_{HS} - f_1 W_{1,HS}}{(1 - f_1)} \tag{3}$$

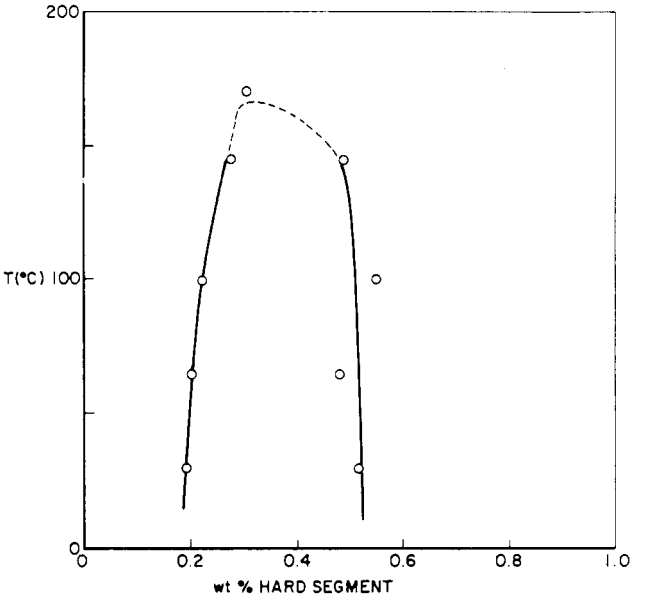

Figure 6. Apparent microphase composition–temperature diagram for PU-30.

where $W_{1,HS}$ and $W_{2,HS}$ are weight fractions of hard segment in the soft-segment-rich and hard-segment-rich microphases, respectively, and W_{HS} is the overall hard-segment content of the specimen. The overall weight fraction of the soft-segment-rich microphase is given by

$$f_1 = \frac{\Delta C_{p1}}{\Delta C_p{}^0{}_{SS}(1 - W_{1,HS}) + \Delta C_p{}^0{}_{HS}(W_{1,HS})} \tag{4}$$

ΔC_{p1} is the measured heat capacity change at the soft microphase T_g and has the units of cal/g of total polymer.

The microphase composition–temperature diagram for PU-30 shown in Figure 6 is calculated from these relations assuming that $\Delta C_p{}^0{}_{HS} = 0$. The degree of intersegmental mixing is substantial in both microphases and increases with increase in annealing temperature. The MST occurs between 145 and 175 °C. The transition to the homogeneous phase is also indicated in the thermograms for annealing temperatures above 145 °C. These thermograms exhibit phase-separation exotherms visible near 60 °C in Figure 4. The composition–temperature diagram does not depend strongly on the value assumed for $C_p{}^0{}_{HS}$ in eq 4. If the Simha–Boyer rule is invoked, for example, ($\Delta C_p{}^0{}_{HS} \simeq 0.07$ cal/g) the soft-microphase compositions remain unchanged and the hard-microdomain compositions are changed by roughly 10% (becoming less pure).

The thermograms for PU-30 exhibit only two weak endotherms, which are denoted by the arrows in Figure 4. A high-temperature microcrystalline-melting endotherm is absent for this material. A map of the approximate peak endotherm temperatures as a function of annealing temperature appears in Figure 7. The low-temperature endotherm, T_I, occurs ca. 20 °C above T_a, consistent with previous investigations.[19,20,22] The higher temperature endotherm, T_{II}, rises asymptotically to a value of ca. 170 °C until the curve intersects the $T_m = T_a$ line. T_{II} then drops to ca. 160 °C and is independent of further increase in T_a. Comparison of this behavior with the composition–temperature diagram (Figure 6) reveals that this discontinuity in endotherm temperatures is coincident with the MST process. The origin of the T_{II} endotherm is therefore related to the microphase separation transition, that is, to the onset of intersegmental mixing leading to disruption of the microdomain structure.

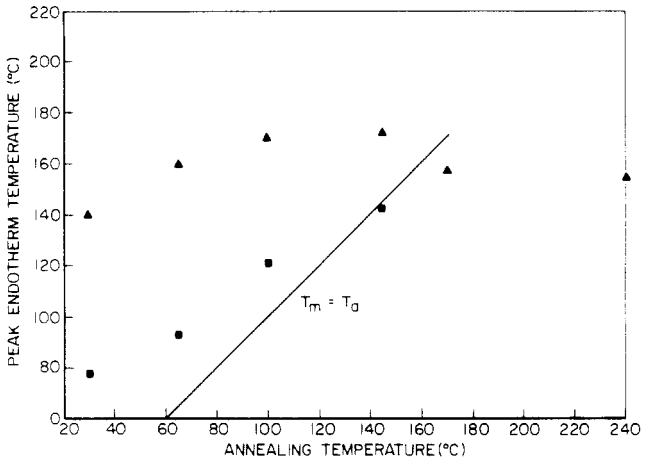

Figure 7. Peak endotherm temperatures as a function of annealing temperature for PU-30: (■) T_I; (▲) T_{II}.

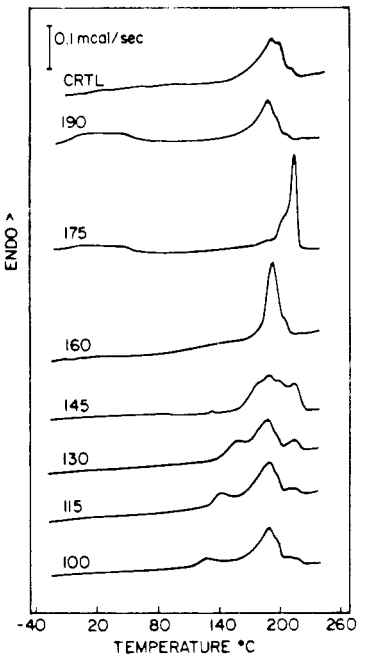

Figure 8. PU-50 thermograms as a function of annealing temperature.

B. PU-50 Annealing Study. DSC thermograms for PU-50 are found to be dependent on the programmed temperature rate. A program rate of 40 °C was therefore selected in order to minimize the occurrence of structural reorganization during the DSC scan. DSC thermograms for various annealing conditions are shown in Figure 8. Below T_a = 160 °C, three characteristic endotherms are visible. These endotherms shift to higher temperatures and merge into a single peak as T_a is increased to 175 °C. At higher annealing temperatures, the thermograms show a single broad endotherm that is shifted to lower temperatures and is insensitive to the annealing temperature. The magnitude of the low temperature T_I endotherm is a function of the annealing time, as documented by the data for annealing at 100 °C contained in Figure 9. At this annealing temperature, the higher temperature endotherms appear to be independent of annealing time. Similar behavior has been reported by Cooper et al.[20,22]

Measurements at additional annealing temperatures were carried out in order to elucidate the origins of the T_{II} and T_{III} endotherms. These results (Figure 10) illustrate that DSC endotherms are sensitive to annealing temperature changes of the order of 5 °C. A compilation of the

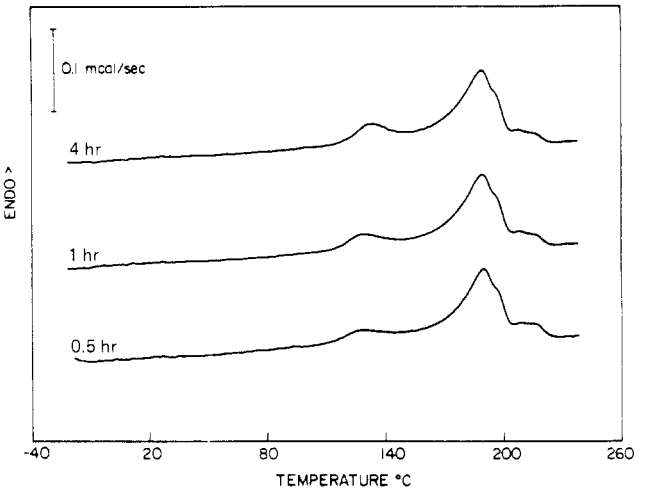

Figure 9. Time dependence of the low-temperature endotherm (T_I) for PU-50 annealed at 100 °C.

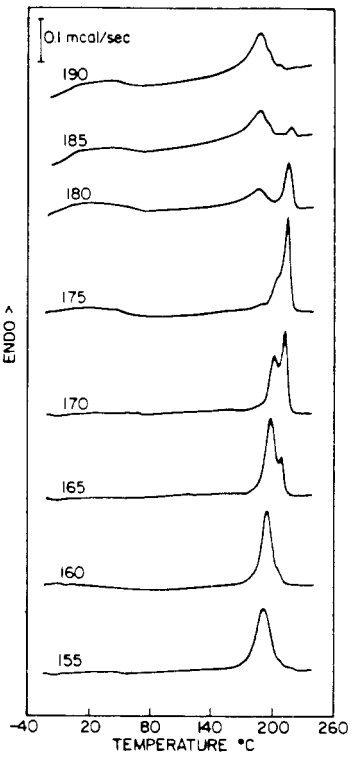

Figure 10. PU-50 thermograms as a function of annealing temperature.

peak endotherm temperatures is given in Figure 11. The low-temperature endotherm (T_I) occurs 20–30 °C above T_a and merges with the T_{II} endotherm to form a single T_{II} peak at $T_a \cong 155$ °C. The T_{II} endotherm remains relatively unchanged below $T_a \cong 145$ °C and then begins to rise in temperature and decrease in magnitude at the expense of the T_{III} endotherm. The peaks finally merge at $T_a \cong 175$ °C. As the annealing temperature is raised above 175 °C, the T_{III} endotherm first diminishes concurrent with the reappearance of an apparent T_{II} endotherm and then essentially vanishes for $T_a \cong 190$ °C and above. The peak endotherm data can be categorized qualitatively into three regimes of behavior depending upon the annealing temperature, as denoted on Figure 11.

Region 1. For annealing temperatures up to ca. 150 °C, a strong crystalline endotherm is absent, and the peak endotherm behavior for PU-50 is similar to that of PU-30 (see Figure 7). Crystalline wide-angle X-ray diffraction

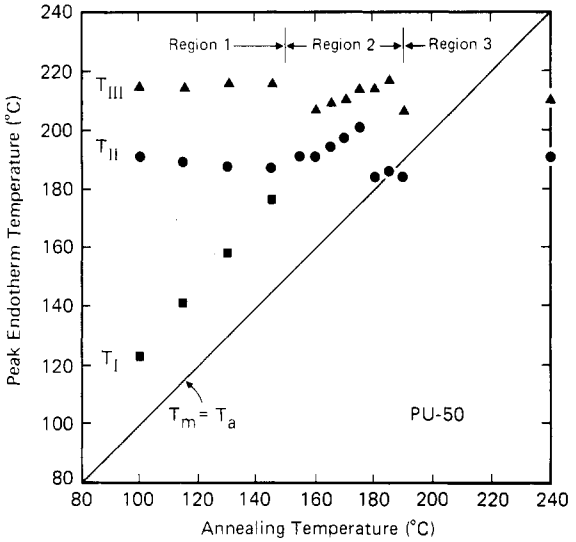

Figure 11. Endothermic transition temperatures for PU-50 as a function of annealing temperature: (■) T_I peak; (●) T_{II} peak; (▲) T_{III} peak.

(WAXD) peaks are also absent in specimens annealed under these conditions.[39] Phase separation occurs rapidly at these temperatures. Crystallization, however, is diffusion-controlled near the hard segment T_g (110 °C), and the finite annealing time is not sufficient to develop significant crystallinity. The small T_{III} endotherm observed may reflect crystallization that occurred during the DSC scan. The high-temperature endothermic response is therefore insensitive to the precise annealing temperature. Assuming that PU-50 behaves in a manner analogous to that of PU-30, it follows that the origin of the T_{II} endotherm may be assigned to the MST process. The apparent MST temperature is approximately 185 °C, given by the intersection of the T_{II} line in region 1, with the $T_m = T_a$ line. Simultaneous SAXS–DSC measurements described in the paper that follows confirm this assignment.[40]

Region 2. The distinguishing feature of region 2 behavior is the development of hard-segment crystallinity. As the temperature is raised within this temperature range, increased crystallinity levels are indicated by increases in the overall endotherm enthalpy and by WAXD experiments.[39] This increase is expected to occur in the diffusion-controlled regime of crystallization due to the increased mobility at higher temperatures.[41]

The development of crystallinity brings about a gradual shift in the endothermic response from a single T_{II} peak for T_a = 155 °C to a single T_{III} peak for T_a = 175 °C. The origin of the latter endotherm can therefore be ascribed to the melting of crystalline hard segments. The increase in crystallinity is also accompanied by continued elevation in the peak temperatures of both the T_{II} and T_{III} endotherms.

Region 3. The onset of region 3 behavior is marked by a discontinuity in the DSC response between annealing temperatures of 175 and 190 °C (see Figure 10). As T_a is raised above 175 °C, the T_{III} endotherm diminishes in magnitude while the T_{II} endotherm reappears at temperatures similar to those found in region 1. The observed decrease in the level of crystallinity is expected for lower undercoolings when crystallization is nucleation-controlled.[41]

The discontinuity in behavior between regions 2 and 3 is a direct consequence of the microphase separation transition, which was previously inferred to occur at ~185 °C for PU-50. Above the MST temperature (i.e., in region 3), the microdomain structure is unstable, and crystallization takes place from the homogeneous mixed melt phase. This in a sense might be termed a "solution" crystallization process. Real-time SAXS-DSC experiments show that crystallization in this region occurs slowly with induction periods of the order of 30 min.[42]

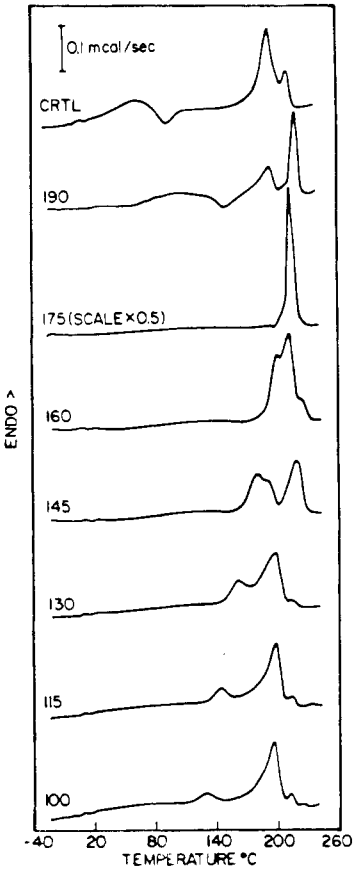

Figure 12. PU-70 thermograms as a function of annealing temperature.

Region 2, in contrast, is below the MST temperature, and the microdomain structure is stable. Phase separation occurs in roughly 10 min for these temperatures, as determined by torsion braid analysis,[40] and presumably precedes crystallization. In this case, crystallization must occur within the confines of existing hard microdomains, by what might be termed a form of "bulk" crystallization. It is this difference in the morphological environments for crystallization that gives rise to the observed differences in endothermic response between regions 2 and 3.

C. PU-70 Annealing Study. Thermograms for PU-70 after annealing at a variety of temperatures are shown in Figure 12. The basic behavior is qualitatively similar to that of PU-50. Region 1 response is obtained for $T_a < 140$ °C, where three characteristic endotherms are again observed. The T_I endotherm is found at temperatures about 30–40 °C higher than the annealing temperature. T_{II} endotherms occur at ca. 190 °C, suggesting that this is the MST temperature for PU-70. The presence of only weak T_{III} endotherms indicates that significant crystallinity does not develop under region 1 conditions.

For T_a = 145 °C, region 2 behavior similar to that of PU-50 is observed. Increased crystallinity is indicated by the growth of the T_{III} endotherm and is accompanied by a slight increase in the melting temperature. At T_a = 160 °C, however, the behavior departs dramatically from that of PU-50. The magnitude of the T_{III} endotherm decreases drastically, and a new endotherm with depressed melting temperature (ca. 215 °C) appears. At T_a = 175 °C, the endotherms merge into a strong and extremely sharp peak

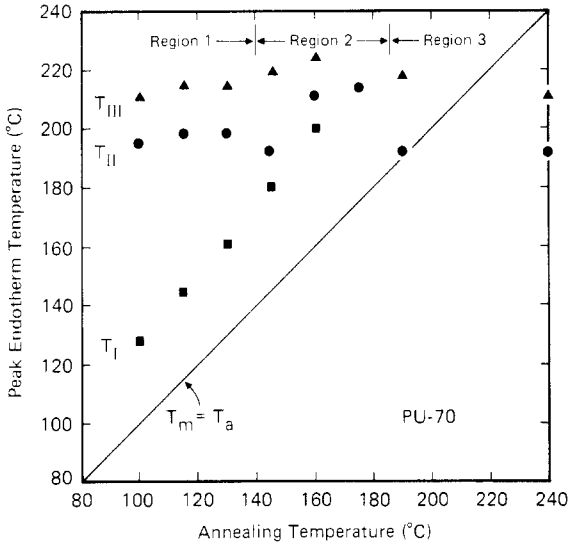

Figure 13. Endothermic transition temperatures for PU-70: (■) T_I peak; (●) T_{II} peak; (▲) T_{III} peak.

at this same temperature (215 °C). WAXD experiments suggest that the emergence of this peaks may be associated with the development of a second MDI–BD crystal form.[39] Although a full discussion of this behavior is beyond the scope of the present article, it can be generally stated that the overall degree of crystallinity increases within region 2, as was found for PU-50.

Region 3 response occurs for temperatures above the MST temperature (ca. 190 °C). Thermograms in this region show an exotherm resulting from phase separation of the frozen-in homogeneous phase. The magnitude of the T_{III} endotherm diminishes while that of the T_{II} endotherm increases, consistent with the decreased crystallization rate at lower undercoolings.

Most of the thermograms for PU-70 present a feature near 70 °C that appears to be a glass-transition process. The low ΔC_p value for this transition (~0.02 cal/g) suggests that it may correspond to a hard microdomain T_g. Detailed analysis of this transition was not undertaken due to the low ΔC_p value and subsequent difficulty in observing the transition.

Summary

DSC annealing experiments have been used to probe the temperature dependence of microphase separation and multiple endothermic response is segmented block copolyurethanes. DSC thermograms for materials of low hard-segment content exhibit two characteristic endotherms. A third endotherm appears for samples containing sufficient hard-segment content to allow hard-segment crystallization. The positions of these endotherms are sensitive to annealing temperature changes of as little as a few degrees Centigrade.

The low-temperature T_I endotherms appear at temperatures that are 20–40 °C above the annealing temperature. For a fixed annealing temperature, the peak temperature of this endotherm is found to increase with increase in the hard-segment content. The peak magnitude is shown to be time dependent, increasing slowly during the annealing process. This time dependence is consistent with the previous suggestion[19,20,22] that the endotherm is associated with a local reorganization within the hard microdomains. The precise origin of the T_I endotherm remains unknown however.

The intermediate-temperature T_{II} endotherm has previously been attributed to the disruption of long-range order of an unspecified nature. Measurements of the ΔC_p and T_g of specimens quenched from various annealing temperatures demonstrate that this endotherm is associated with the disruption of microdomain structure that occurs at the microphase separation transition (MST) temperature. This interpretation is confirmed by the simultaneous SAXS–DSC experiments described in the following paper.[40] Under annealing conditions that are unfavorable for hard-segment crystallization, the MST temperature increases with the hard-segment content. In comparison, the MST temperature for diblock copolymers is predicted to be a function of the copolymer sequence length.[43-45] The increase in the MST temperature may therefore be a consequence of the increase in the average hard-segment sequence length as the hard-segment content is increased.[46]

It is also possible, however, that the intermixing of hard and soft segments occurs instantaneously upon melting of a disordered crystalline hard-segment polymorph. Disordered polymorphs of MDI–BD have been reported in similar polyurethanes[47,48] and have recently been observed in studies of the pure MDI–BD hard segment.[49] The existence of a disordered hard-segment crystal form would also account for the observed T_{II} increase with hard-segment content. In this case, the T_{II} melting-temperature increase would follow from the Flory melting-point relation[50] as the sequence length increased. This relation has been found to be adequate in describing the composition dependence of hard-segment melting points in 2,6-toluene diisocyanate polyurethanes.[10]

The T_{III} endotherm results from the melting of microcrystalline hard segments. For all annealing conditions, the T_{II} endotherm, if observed, occurs prior to this endotherm, implying that disruption of the disordered crystalline and/or noncrystalline hard microdomains precedes melting of the microcrystalline hard segments.

The annealing temperature dependence of the DSC endotherms falls generally into three regimes of behavior. For annealing temperatures above the MST, crystallization of the hard segments occurs from a homogeneous mixed "solution" of hard and soft segments. The level of crystallinity under these conditions is controlled by the undercooling, and the peak endotherm temperatures are insensitive to the annealing temperature.

Two regimes of behavior are seen for annealing temperatures below the MST. At temperatures sufficiently above the hard-microdomain glass transition, crystallization can occur. Crystallization appears to be diffusion-controlled within this region, as evidenced by a continual increase in the endotherm enthalpy as the annealing temperature is raised. The development of crystallinity is generally accompanied by gradual elevation in the T_{II} and T_{III} peak endotherm temperatures, although the behavior of PU-70 is more complex. Crystallization at temperatures below the MST probably occurs within the confines of the preexistent microdomain structure and might be classified as a "bulk" process.

A third region of behavior is observed for lower annealing temperatures approaching the hard microdomain T_g. Within this region, the T_{III} endotherm is weak, indicating that crystallinity is essentially absent, and the T_{II} and T_{III} endotherm temperatures are relatively constant. The differentiation, by level of crystallinity, of two behavioral regimes below the MST is somewhat artificial in that crystallization is apparently diffusion-controlled in both regions of annealing temperature. The distinction between behaviors is useful, however, in discussing the peak endotherm temperature response. Furthermore, the T_I endotherm is no longer observable at annealing temperatures

where crystallinity is developed, providing some concrete basis for differentiating the two regions.

In the paper that follows, the morphological changes that accompany these changes in thermal properties are studied by simultaneous SAXS–DSC measurements. A more detailed discussion of the peak endotherm temperature trends and the consequences of this behavior in terms of structure–property relations is presented therein.

Acknowledgment. We wish to acknowledge partial support of this project by a grant from the Dow Chemical Co. Foundation and National Science Foundation Grant No. DMR-81054612 administered through the Polymer Program of the Division of Materials Research. The thermal analysis equipment was procured with the aid of NSF equipment grant DMR-8206187. Finally, we would like to thank Dr. R. Zdrahala, formerly of the Union Carbide Corp., for supplying the samples for experimental study and Dr. T. P. Russell for his helpful comments during the preparation of this manuscript.

Registry No. (MDI)·(BD)·(methyloxirane)·(oxirane) (copolymer), 34407-15-3.

References and Notes

(1) Bonart, R.; Muller, E. H. *J. Macromol. Sci., Phys.* **1974**, *B10*, 177.
(2) Bonart, R.; Muller, E. H. *J. Macromol. Sci., Phys.* **1974**, *B10*, 345.
(3) Schneider, N. S.; Desper, C. R.; Illinger, J. L.; King, A. O.; Barr, D. *J. Macromol. Sci., Phys.* **1975**, *B11*, 527.
(4) Van Bogart, J. W.; Gibson, P. E.; Cooper, S. L. *J. Polym. Sci., Polym. Phys. Ed.* **1983**, *21*, 65.
(5) Koberstein, J. T.; Stein, R. S. *J. Polym. Sci., Polym. Phys. Ed.* **1983**, *21*, 1439.
(6) Leung, L. M.; Koberstein, J. T. *J. Polym. Sci., Polym. Phys. Ed.* **1985**, *23*, 1883.
(7) Abouzahr, S.; Wilkes, G. L.; Ophir, Z. *Polymer* **1982**, *23*, 1077.
(8) Ophir, Z.; Wilkes, G. L. *J. Polym. Sci., Polym. Phys. Ed.* **1980**, *18*, 1469.
(9) Paik Sung, C. S.; Hu, C. B.; Hu, C. S. *Macromolecules* **1980**, *13*, 111.
(10) Senich, G. A.; MacKnight, W. J. *Adv. Chem. Ser.* **1979**, *176*, 97.
(11) Brunette, C. M.; Hsu, S. L.; MacKnight, W. J.; Schneider, N. S. *Polym. Eng. Sci.* **1981**, *21*, 163.
(12) Huh, D. S.; Cooper, S. L. *Polym. Eng. Sci.* **1971**, *11*, 369.
(13) Ng, H.; Allegrezza, A. E.; Seymour, R. W.; Cooper, S. L. *Polymer* **1973**, *14*, 255.
(14) Illinger, J. I.; Schneider, N. S.; Karasz, F. E. *Polym. Eng. Sci.* **1972**, *12*, 25.
(15) Samuels, S. L.; Wilkes, G. L. *J. Polym. Sci., Polym. Symp.* **1973**, *43*, 149.
(16) Zdrahala, R. J.; Critchfield, F. E.; Gerkin, R. M.; Hager, S. L. *J. Elastomers Plast.* **1980**, *12*, 184.
(17) Kajiyama, T.; MacKnight, W. J. *Macromolecules* **1969**, *2*, 254.
(18) Kajiyama, T.; MacKnight, W. J. *Trans. Soc. Rheol.* **1969**, *13*(4), 527.
(19) Seymour, R. W.; Cooper, S. L. *Macromolecules* **1973**, *6*, 48.
(20) Hesketh, T. R.; Van Bogart, J. W. C.; Cooper, S. L. *Polym. Eng. Sci.* **1980**, *20*, 190.
(21) Schneider, N. S.; Paik Sung, C. S.; Matton, R. W.; Illinger, J. L. *Macromolecules* **1975**, *8*, 62.
(22) Van Bogart, J. W. C.; Bluemke, D. A.; Cooper, S. L. *Polymer* **1981**, *22*, 1428.
(23) Schneider, N. S.; Paik Sung, C. S. *J. Polym. Sci., Polym. Chem. Ed.* **1977**, *17*, 73.
(24) Camberlin, Y.; Pascault, J. P. *J. Polym. Sci., Polym. Chem. Ed.* **1983**, *21*, 415.
(25) Paik Sung, C. S.; Schneider, N. S. *Macromolecules* **1975**, *8*, 68.
(26) Jacques, C. H. M.; "Polymer Alloys"; Klempner, D.; Frisch, K. C. Eds.; Plenum Press: New York, 1977; p 287.
(27) Perkin-Elmer Instruction Manual for Model DSC-4, 0993-9666, pp 3–12 (Rev. May 1982).
(28) Wood, L. A. *J. Polym. Sci.* **1958**, *28*, 319.
(29) Fox, T. G. *Bull. Am. Phys. Soc.* **1956**, *50*, 549.
(30) MacKnight, W. J.; Yang, M.; Kajiyama, T. *Polym. Prepr. (Am. Chem. Soc., Div. Polym. Chem.)* **1968**, *9*(1), 860.
(31) Couchman, P. R. *Macromolecules* **1978**, *11*, 117.
(32) Simha, R.; Boyer, R. F. *J. Chem. Phys.* **1972**, *37*, 1003.
(33) Brunette, C. M.; Hsu, S. L.; MacKnight, W. J. *Macromolecules* **1982**, *15*, 71.
(34) Coleman, M. M.; Skrovanek, D. J.; Howe, S. E.; Painter, P. C. *Macromolecules* **1985**, *18*, 299.
(35) Wilkes, G. L.; Emerson, J. A. *J. Appl. Phys.* **1976**, *47*(1), 4261.
(36) Wilkes, G. L.; Bagrodia, W.; Humphries, W.; Wildenauer, R. *J. Polym. Sci. Polym. Lett.* **1975**, *13*, 321.
(37) Ophir, Z.; Wilkes, G. L. *Adv. Chem. Ser.* **1979**, *176*, 53.
(38) Wilkes, G. L.; Wildenauer, R. *J. Appl. Phys.* **1975**, *46*(10), 4148.
(39) Galambos, A.; Koberstein, J. T. *Bull. Am. Phys. Soc.* **1985**, *30*(3), 444.
(40) Koberstein, J. T.; Russell, T. P. *Macromolecules*, following paper in this issue.
(41) Hoffman, J. D.; Davis, G. T.; Lauritzen, J. I., Jr. "Treatise on Solid State Chemistry"; Hannay, N. B., Ed.; Plenum Press: New York, 1976.
(42) Koberstein, J. T.; Russell, T. P. unpublished data.
(43) Krause, S. *Macromolecules* **1970**, *3*, 84.
(44) Meier, D. J. *J. Polym. Symp.* **1969**, *C26*, 81.
(45) Leibler, L. *Macromolecules* **1980**, *13*, 1602.
(46) Peebles, L. H., Jr. *Macromolecules* **1974**, *7*, 872; **1976**, *9*, 58.
(47) Briber, R. M.; Thomas, E. L. *J. Macromol. Sci., Phys.* **1983**, *B22*(4), 509.
(48) Blackwell, J.; Lee, C. D. *J. Polym. Sci., Polym. Phys. Ed.* **1984**, *22*, 759.
(49) Macosko, C. W., private communication.
(50) Flory, P. J. "Principles of Polymer Chemistry"; Cornell University Press: Ithaca, NY, 1953; p 570.